P2F.3 FORMULA FOR SPIRAL CLOUD-RAIN BANDS OF A TROPICAL CYCLONE

Boris S. Yurchak*
University of Maryland, Baltimore County, Greenbelt, Maryland

1. INTRODUCTION

Spiral cloud-rain bands (SCRB) are some of the most distinguishing features inherent in satellite and radar images of tropical cyclones (TC). The finding of reliable indicators of the TC's intensity and its center location is one of the fields in SCRB study. The kind of function that is most fitting for description of an SCRB is an important point in such research. This problem is directly connected with the mechanism of SCRB formation and evolution. In the current work, the simplest hypothesis of entrapment of cloud masses was used. The core of this hypothesis is an assumption that clouds are involved by the spiral wind streamlines flown into the center of a cyclone.

2. EQUATION FOR WIND STREAMLINE IN TC

According to Mamedov and Pavlov (1974), the streamline equation in a polar coordinate system can be written as

$$r\frac{d\varphi}{u} = \frac{1}{v}dr \quad , \qquad (1)$$

where r is a radius-vector, φ is an angle between radius vector and the positive direction of X, and u and v are tangential (to circular isobar) and radial components of air particle motion, respectively. One of the main parameters of SCRB is the so-called “crossing angle” which is an angle between the tangent to the streamline (cloud track) and the tangent to the circular isobar at a particular point (Fig.1). It is known from many experimental observations, that the crossing angle decreases with the decrease of spiral radius as the point is coming to the pole of a spiral. It also occurs at a fixed distance, due to cyclone intensity increase (Report WMO (1985), Raghavan (2003)). Depending on relations among the parameters presented in the streamline equation (1), a solution of this equation will be some kind of a spiral. In particularly, the logarithmic spiral

$$r = R\cdot\exp(-\varphi\cdot tg\alpha)\,, \qquad (2)$$

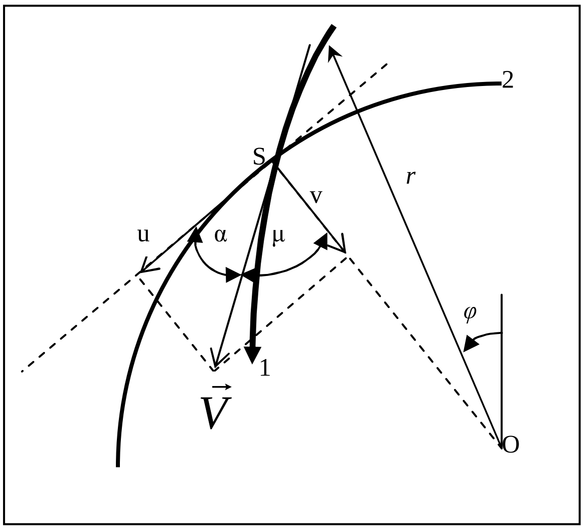

Fig.1. Derivation of the streamline equation for a TC. (*1*) wind streamline; (*2*) circular isobar; *O* is the TC center; *S* is an arbitrary point within a wind streamline; $\vec{V}$ is the tangential wind speed at the point *S*; *u* and *v* are tangential (to circular isobar) and radial components of the tangential wind, respectively; α and μ are the crossing angle and the inflow angle, respectively; φ is the polar angle; and *r* is a radius-vector.

where R is cyclone radius (it is estimated by radius of the last circle isobar of the TC system), φ is spiral's polar angle ($\varphi=0$ at $r=R$), α is crossing angle, means that radial and tangential wind components have the same law of radius dependence (the crossing angle is constant): $v/u=tg\alpha=const$. From the known experimental data, pointed in Weatherford and Gray (1988), for example, it does not point out that the above conditions really might be in TC. The logarithmic spiral expression can be presented also as a dependence of polar angle on radius normalized by R:

$$\varphi = -ctg\alpha\cdot\ln\frac{r}{R} \qquad (3)$$

In the modified logarithmic spiral (Anthes (1982)):

$$\ln\left(\frac{r-r_m}{R}\right) = -\varphi\cdot tg\alpha(r)\,, \qquad (4)$$

where:

$$tg\alpha(r) = tg\alpha_\infty\left(1-\frac{r_m}{r}\right),\; tg\alpha_\infty = tg\alpha(r)_{r\to\infty}\;,$$

**Corresponding author address*: Boris S. Yurchak Univ. of Maryland, Baltimore County, GEST, Greenbelt, MD, 301-614-5670, e-mail: yurboris@umbc.edu

r_m is maximal wind radius and α_∞ is peripheral crossing angle, it is taken into account empirically that the crossing angle decreases as the point approaches the center of TC. But it does not depend on TC intensity as well. Thus, these models of the crossing angle change have adjusting and empirical style, and the application of such or other spiral form is not substantiated.

3. STREAMLINE EQUATION TAKING INTO ACCOUNT THE CHANGES OF THE INFLOW ANGLE AS A FUNCTION OF TC RADIUS

Steady-state air motion in the cyclone causes the friction force $F_{fr} = -kV$, where k is a friction factor. In accordance with Guralnik et al. (1972), the deviation angle to the right from the gradient force directed to the cyclone center (Fig. 1) is given by an expression

$$tg\mu(r) = \frac{l}{k} + \frac{V(r)}{kr}, \qquad (5)$$

where $l = 2\omega \sin\phi$ is the Coriolis parameter (ω is the angular speed of the Earth rotation, ϕ is the altitude) and V is the modulus of particle's speed vector. As follows from the Fig.1, the crossing angle and inflow angle are connected by a relationship

$$\alpha + \mu = \frac{\pi}{2} \qquad (6)$$

whence

$$tg\alpha(r) = ctg\mu(r) = \frac{k}{l + \frac{V(r)}{r}} = \frac{k}{l} \cdot \frac{1}{1 + \frac{V(r)}{r \cdot l}} \qquad (7)$$

The values of the crossing angle are provided in Table 1 for different rations between the Coriolis parameter and parameter $\frac{V(r)}{r}$.

Table 1. The crossing angle values depending on relationship between the parameters of formula (7)

$\frac{V(r)}{l \cdot r}$	~0	1	2	5	10	20	50	100
$\alpha(r)^0$	59	40	29	16	9	5	2	~0

In calculation of Table 1, the Coriolis parameter was chosen for latitude of 19^0, i.e. $l = 2\omega\sin\phi = 4{,}8 \cdot 10^{-5} s^{-1}$, and friction factor $k \approx 8 \cdot 10^{-5} s^{-1}$. The data of Table1 show that the range of the crossing angle is from 0 to 40 degrees, which is in accordance with the values observed experimentally (Report WMO (1985)). Because the increase in the ratio of wind speed to radius causes the decrease in the crossing angle, it is possible to conclude that the current model of the crossing angle change is matched qualitatively to the experimental data (the crossing angle decreases when the point approaches the center of a TC and due to TC intensity increase). Solution of the equation (1) with $\frac{u}{v} = tg\mu$, where $tg\mu$ is defined by equation (5), and the speed of wind changes with cyclone radius is in accordance with the power low (Anthes (1982))

$$V(r) = V_m \left(\frac{r_m}{r}\right)^n \qquad (8)$$

is derived by Yurchak (2007) and has a form:

$$\varphi = A \cdot \left(\frac{1}{y^{n+1}} - 1\right) - B \cdot \ln y, \qquad (9)$$

where $y = \frac{r}{r_0}$ is a relative radius, $A = \frac{y_m^n}{k\tau(n+1)}$, $B = \frac{l}{k}$, $y_m = \frac{r_m}{r_0}$, $\tau = \frac{r_0}{V_m}$.

Equation (9) can be represented in the exponent-logarithmic form as well:

$$\varphi = A \cdot \left\{ e^{-(n+1)\ln y} - 1 \right\} - B \cdot \ln y \qquad (9a)$$

3. CROSSING ANGLE OF THE HYPERBOLIC-LOGARITHMIC SPIRAL

It is easy to show based on (7) that, in contrast to the logarithmic spiral, the crossing angle of HLS depends on TC radius:

$$tg(\alpha(r)) = \frac{k}{l} \cdot \frac{1}{1 + Ro \cdot \left(\frac{r_m}{r}\right)^{n+1}} \qquad (10)$$

where $Ro = \frac{V_m}{r_m \cdot l}$ is the Rossby number.

Expression (10) can also be written as a function of HLS parameters:

$$tg(\alpha(y)) = \frac{1}{B + A \cdot \frac{n+1}{y^{n+1}}} \qquad (11)$$

As detailed in (11), particularly, the coefficient A has a notably greater "weight" than the coefficient B as the point approaches the cyclone center (with decreasing y). This feature, as it will be shown below, is the factor which governs mainly the difference between HLS and the logarithmic spiral within the central part of TC.

4. COMPARISON OF THE LOGARITHMIC AND HYPERBOLIC-LOGARITHMIC SPIRALS

For illustration, several HLSs in polar and Cartesian semi-logarithmic (*φ*-*lny*) coordinates are shown in Fig.2 with parameters: n=0.5, V_m=40 m/s and 80 m/s, r_m=40 km, r_o=400 km, and k=l. At that A=4.374 and A=8.75 respectively and B=1. It is easy to show that the logarithmic spiral with the most applicable crossing angle of 18^0 (Willoughby (1978)) is the specific case of the HLS with A = 0 and B = 3.077. This spiral is also shown in Fig.2 for comparison. The increase of the factor A is due to increasing TC intensity under a constant exponent and leads to the "rounding" of the spiral (decreasing of crossing angle). This is in accordance with (11) as well. It is possible to show also that the change by twice of the factor B at the logarithmic component of the HLS and the exponent n practically does not impact the shape of the HLS. With A=0, the HLS degenerates to the classical logarithmic spiral where $tg\,\alpha = B^{-1}$. Main difference between HLS and the logarithmic spiral is indicated in the central part of a TC. The logarithmic spiral goes to the center much faster then the HLS. The HLS seems like curve around the TC's eye. At that, the "roundness" of this curling is so much the better as the intensity is higher.

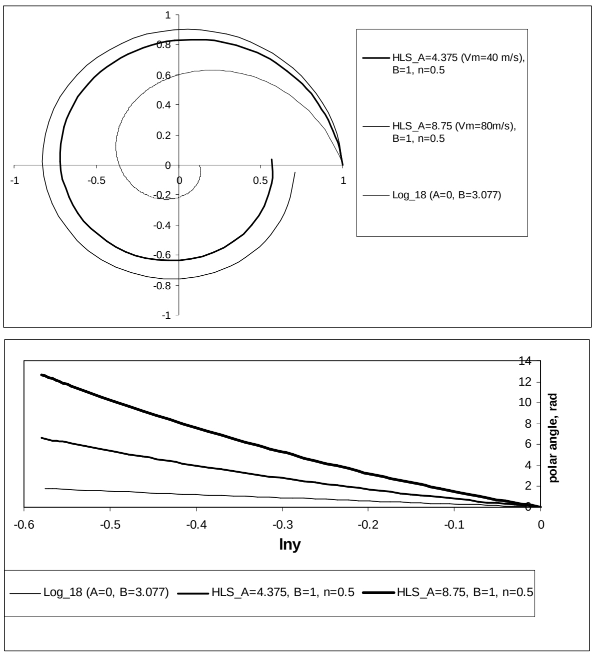

Fig.2. Hyperbolic-logarithmic spiral in polar (top plot) and semi-logarithmic (bottom plot) coordinates with different parameters. Log_18 is the logarithmic spiral with 18^0 crossing angle.

5. SOME EXAMPLES OF APPROXIMATION OF SPIRAL CLOUD-RAIN BANDS IN A TROPICAL CYCLONE BY A HYPERBOLIC-LOGARITHMIC SPIRAL

To illustrate the practical applicability of the proposed way of SCRB description, the approximation of spiral bands of satellite and radar images of TCs was conducted for several examples. To calculate the HLS and the logarithmic spiral parameters, the least-squares method was applied. An approximation was done in accordance with a rapid design scheme under the assumption of the constant exponent n equal to 0.5. The processing results of TC "Mitag" (UK MetOffice, archive of TC images: http://www.metoffice.com/weather/tropicalcyclone/images.html) and radar images of TC "Irving" (Yurchak (1997)) are provided in Figs.3-5 and Table 2. Other examples of HLS application for SCRB approximation and for a more exact location of a TC center are provided in Yurchak (2007).

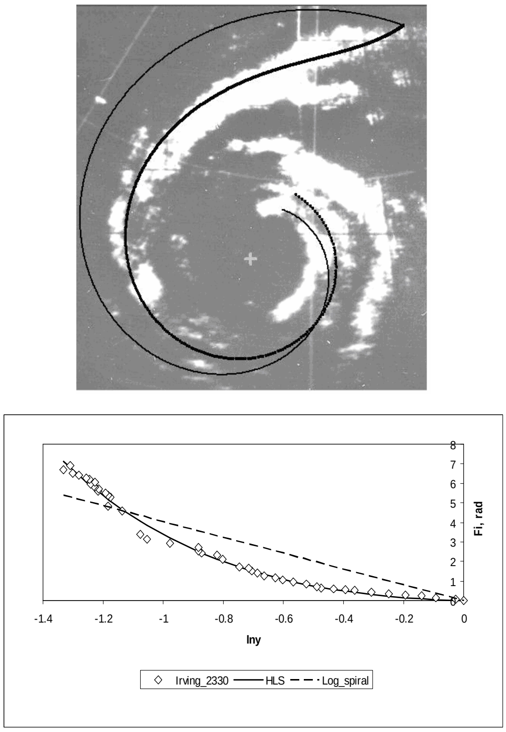

Fig.3. Example of comparative approximation of the principal spiral band of TC "Irving" at 23:30 (07/23/89) by logarithmic spiral and HLS. Image at the top is original radar image, bottom plot is spiral band points and its approximation by HLS and logarithmic curves in semi-logarithmic coordinates. Logarithmic spiral is denoted by thin line on radar image and by dashed line on approximation plot (bottom). Parameters of HLS are A=1.51, B=-1.57. Parameter of the logarithmic spiral is B_L=4.048.

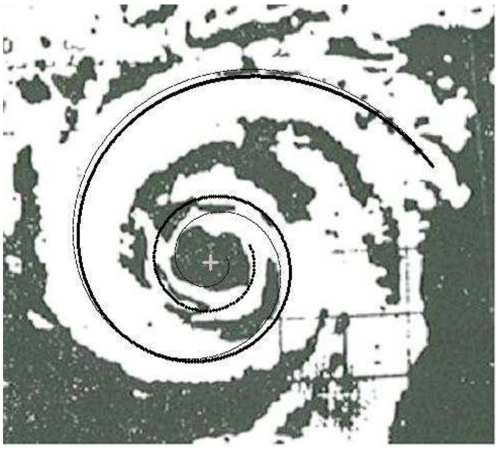

Fig.4. Approximation of the principal cloud-rain band of TC "Irving" at 4:31am (07/24/89) by two turns of HLS (bold line) and the logarithmic spiral (thin line). Main difference between the spirals is observed close to the center of TC. Parameters of the spirals are listed in Table 2.

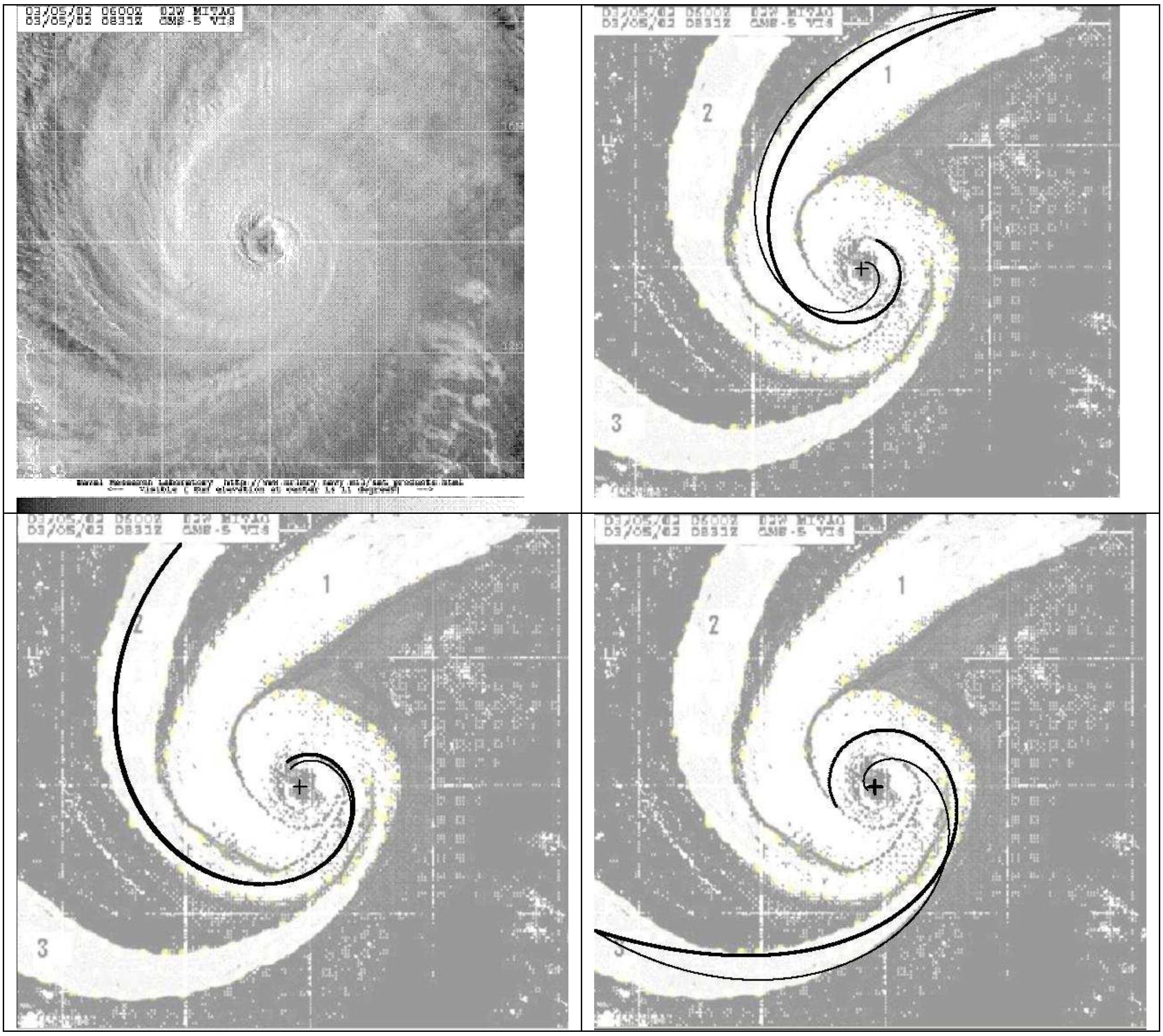

Fig.5. Approximation of three spiral cloud-rain bands of TC "Mitag" by one turn of logarithmic (thin line) and HLS (bold line) spirals. Top left picture is an original image (source: UK MetOffice]. Edited spiral cloud-rain bands are annotated by numbers: 1 is principal band, 2 and 3 are secondary bands. Parameters of spirals are listed in Table 2.

Table 2. Results of approximation of the spiral cloud-rain bands by hyperbolic-logarithmic and logarithmic spirals of several examples of satellite and radar measurements of TCs

TC name, Date, (Reference)	Number of a spiral	Parameters of the HLS					Parameters of the logarithmic spiral			Residual variance ratio
		A	σ_A	B	σ_B	Residual variance	B_L	σ_{B_L}	Residual variance	
MITAG, 03/05/2002 GMS-5 (UK MetOffice)	1	0.16	0.02	0.95	0.08	0.1404	1.75	0.1	0.2839	0.49
	2	0.04	0.01	2.28	0.06	0.0770	2.44	0.03	0.0849	0.91
	3	0.27	0.04	0.57	0.15	0.1236	1.65	0.09	0.2125	0.58
IRVING, 07/24/1989, 04:31am, MRL-5 (Yurchak (1997))		1.25	0.26	1.04	0.76	0.4736	4.7	0.26	0.5656	0.84

6. SUMMARY

In this paper, a physically substantiated formula for spiral cloud-rain bands of TC based on the physical approach utilization of the law of inflow angle dependence in TC on its radius is presented. The main feature of the HLS is the dependence of its coefficients on the physical parameters of TC and the environment. The hyperbolic-logarithmic spiral obtained includes the known logarithmic spiral as a specific case. Main advantage of the HLS over the empirical logarithmic approximation is in more exact description of the central part of a TC's spiral cloud-rain complex. There is a base to propose that the obtained formula might be used also for approximation of streamline by processing the radar wind field measurement data (Tuttle and Gall (1999)) to locate more exactly the TC's eye center position.

7. REFERENCES

R. Anthes, *Tropical Cyclones. Their Evolution, Structure and Effects*. AMS, Meteorological Monographs, No. 41, 1982.

I. Guralnik, Dubinskii, G.P., and S. V. Mamikonova, *The Meteorology*. Handbook for Universities, Gidrometeoizdat, Leningrad, 1972 (in Russian).

E. Mamedov and N.I.Pavlov, *Typhoons.* Gidrometeoizdat, Leningrad, 1974 (in Russian).

S. Raghavan, 2003, *Radar Meteorology*. Kluwer Academic Publishers, 2003.

Report of the Seminar on the Application of Radar Data to Tropical Cyclone Forecasting. Tropical Cyclone Programme, Report No. TCP-19, Bangkok, Thailand 21 Nov.–2 Dec., 1983, WMO, Geneva, Switzerland, 1985.

Weatherford, C.L., and W. M. Gray, 1988: Typhoon Structure as Revealed by Aircraft Reconnaissance. Part I: Data Analysis and Climatology. *Mon. Wea. Rev.,* 116, 1032-1043.

Willoughby, H.E., 1978: A Possible Mechanism for the Formation of Hurricane Rainbands. *J. Atmos. Sci.,* 35, 838-848.

Tuttle, J., and R.Gall, 1999: A single-Radar Technique for Estimating the Winds in Tropical Cyclones. *BAMS*, vol. 80, No. 4, 653-668.

Yurchak, B.S., 1997: Radar Study of the Eye of Tropical Cyclone Irving Passing over the Gulf of Tonkin. *Russian Meteorology and Hydrology*, No.6, 17-32 (in Russian).

Yurchak, B.S., 2007: Description of Cloud-Rain Bands in a Tropical Cyclone by a Hyperbolic-Logarithmic Spiral. *Russian Meteorology and Hydrology,* vol. 32, No.1, 8-18.